Water Research 268 (2025) 122781

Contents lists available at ScienceDirect

Water Research

journal homepage: www.elsevier.com/locate/watres

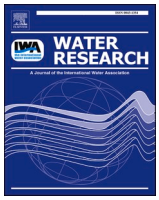

Mechanistic model advancements for optimal calcium removal in water treatment: Integral operation improvements and reactor design strategies

Sergĕj Y.M.H. Seepma [a,c,1,*], Janou A. Koskamp [a], Michel G. Colin [c], Eleftheria Chiou [b,c,2], Rubayat Sobhan [b,c,3], Tim F.J. Bögels [a,c,4], Tom Bastiaan [a,c,5], Hadi Zamanian [c], Eric T. Baars [c], Peter J. de Moel [c,e], Mariëtte Wolthers [a,*], Onno J.I. Kramer [b,c,d,*]

[a] Utrecht University, Department of Earth Sciences, Princetonlaan 8A, 3584, CB Utrecht, the Netherlands
[b] Delft University of Technology, Faculty of Civil Engineering and Geosciences, Department of Water Management, PO Box 5048, 2600, GA, Delft, the Netherlands
[c] Waternet, PO Box 94370, 1090, GJ, the Netherlands
[d] Queen Mary University of London, School of Engineering and Materials Science, Division of Chemical Engineering, Centre for Sustainable Engineering, Mile End Road E1 4NS, London, United Kingdom
[e] Omnisys, Eiberlaan 23, 3871, TG Hoevelaken, the Netherlands

ARTICLE INFO

Keywords:
Plant-Wide integral water treatment
Multiphase flow systems
Fluidized bed reactor
Mechanistic prediction model
Calcium carbonate crystallization and nucleation

ABSTRACT

Drinking water softening has primarily prioritized public health, environmental benefits, social costs and enhanced client comfort. Annually, over 35 billion cubic meters of water is softened worldwide, often utilizing three main techniques: nanofiltration, ion exchange and seeded crystallization by pellet softening. However, recent modifications in pellet softening, including changes in seeding materials and acid conditioning used post-softening, have not fully achieved desired flexibility and optimization. This highlights the need of an integral approach, as drinking water softening is just one step in the drinking water treatment chain, which includes ozonation, softening, biological active carbon filtration (BACF) and sand filtration among others. In addition, pellet softening is often practiced based on operator knowledge, lacking practical key reactor performance indicators (KPIs) for efficient control. For that reason, we propose a newly and improved integral mechanistic model designed to accurately predict (1) calcite removal rates in drinking water through seeded crystallization in pellet softening reactors, (2) the saturation of the filter bed in the subsequent treatment step, (3) values for the KPIs steering the softening efficiency. Our new mechanistic model integrates insights from hydrodynamics, thermodynamics, mass transfer kinetics, nucleation and reactor engineering, focussing on critical variables such as temperature, linear velocity, pellet particle size and saturation index with respect to calcite. Our model was validated with data from the Waternet Weesperkarspel drinking water treatment plant in Amsterdam, The Netherlands, but implies universal applicability for addressing industrial challenges beyond drinking water softening. The implementation of our model proposes five effective KPIs to optimize the softening process, chemical usage, and reactor design. The advantage of this model is that it eliminates the application of numerical methods and fills a significant gap in the field by providing predictions of the carry-over (i.e., the produced $CaCO_3$ fines leaving the fluidized bed) from water softening practices. With our model, the calcium removal rate is predicted with an average standard deviation (SD) of 40 % and the consequential clogging prediction of the BACF bed with an average SD of 130 %. Ultimately, our model provides crucial insights for operational management and decision-making in drinking water treatment plants, steering towards a more circular and environmentally sustainable process.

* Corresponding authors.
E-mail addresses: s.y.m.h.seepma@uu.nl (S.Y.M.H. Seepma), m.wolthers@uu.nl (M. Wolthers), onno.kramer@waternet.nl (O.J.I. Kramer).
[1] IA Group, Geograaf 40, 6921 EW Duiven, the Netherlands.
[2] Hoogheemraadschap van Rijnland, Breestraat 59, 2311 CJ Leiden, the Netherlands.
[3] Deutsche Gesellschaft für Internationale Zusammenarbeit, 89 Gulshan Ave, Simpletree Anarkali, Dhaka, Bangladesh.
[4] Université de Paris, Institut de Physique de Globe de Paris, 75005 Paris, France.
[5] Vitens, Oude Veerweg 1, 8019 BE Zwolle, the Netherlands.

https://doi.org/10.1016/j.watres.2024.122781
Received 3 June 2024; Received in revised form 25 October 2024; Accepted 9 November 2024
Available online 10 November 2024

Nomenclature

Acronyms

AOC	Assimilable organic carbon
BACF	Biological activated carbon filtration
FBR	Fluidized bed reactor
KPI	Key reactor performance indicator
SD	Standard deviation
WPK	Waternet Weesperkarspel drinking water treatment plant in Amsterdam, The Netherlands

Roman Symbols

A_a	Empirical prefactor related to activity calculations $mol^{-1/2}$ $m^{3/2}$
A_r	Total softening reactor cross-sectional area m^2
A_{BACF}	Total BACF reactor cross-sectional area m^2
B_n	Nucleation barrier constant -
a_{sh}, b_{sh}	Sherwood coefficients -
$c_0 - c_4$	Voidage fitting coefficients -
CCPP	Theoretical calcium carbonate precipitation potential mol m^{-3}
$CCPP_{rel}$	Relative theoretical calcium carbonate precipitation potential -
D_f	Diffusion coefficient m^2 s^{-1}
D_r	Cylinder vessel diameter of pellet softening reactor m
d_{ch}	Channel diameter m
d_p	(Average) particle diameter of calcite pellets m
f_a	Activity coefficient -
$f(v_s, h_r)$	Recrystallization factor -
g	Gravitational acceleration constant m s^{-2}
h_{BACF}^{AOC}	BACF bed height saturation by AOC m
$h_{BACF}^{CaCO_3}$	BACF bed height saturation by $CaCO_3$ m
h_r	Fluidized bed height m
I_{tot}	Total ionic strength mol m^{-3}
J_p, J_c, J_n	Precipitation, crystallization, nucleation molar rate mol m^{-3} s^{-1}
k_B	Boltzmann constant m^2 kg s^{-2} K^{-1}
k_f, k_r	Diffusional mass rate constant, surface reaction rate constant m s^{-1}
K_c	Mass transfer coefficient m s^{-1}
K_n	Nucleation rate constant m^{-3} s^{-1}
$K_{sp,\ calcite}$	Solubility product of calcite mol^2 m^{-6}
$K_{sp,\ vaterite}$	Solubility product of vaterite mol^2 m^{-6}
m	Particle mass kg
M_W	Molecular weight kg mol^{-1}
Q_{H_2O}	Water discharge m^3 s^{-1}
r_{aq}	Solution stoichiometry -
$r_{BACF}^{CaCO_3}$	BACF bed height saturation velocity rate m s^{-2}
S_{vat}	Saturation degree of vaterite -
SI_{cal}, SI_{vat}	Saturation index of calcite or vaterite respectively -
SSA_R	Specific surface area per reactor volume m^2 m^{-3}
SSA_W	Specific surface area per water volume m^2 m^{-3}
SSV	Specific space velocity s^{-1}
T	Temperature °C or K
t_r	Reaction time s
v_{BACF}^{AOC}	BACF bed height saturation velocity by AOC m s^{-1}
$v_{BACF}^{CaCO_3}$	BACF bed height saturation velocity by $CaCO_3$ m s^{-1}
v_s	Linear superficial velocity m s^{-1}
V_c	Molecular cluster volume m^3
V_{H_2O}	Water volume m^3
V_m	Molar volume m^3 mol^{-1}

Greek Symbols

β_{gs}	Geometric nuclei shape factor constant -
δ_{fu}	Formula units in a cluster -
ε	Bed voidage -
ε_{BACF}	Voidage of BACF bed -
ε_r	Dielectric constant -
θ	Reaction order coefficient -
μ	Dynamic viscosity kg m^{-1} s^{-1}
ν_k	Kinematic viscosity m^2 s^{-1}
ρ_f, ρ_s	Density of the fluid or solid respectively kg m^{-3}
σ	Standard deviation -
σ_s	Specific surface free energy kg s^{-2}
τ_r	(Average) water residence time s
χ_s	Particle shape factor -

Dimensionless Numbers

Fr_p	Densimetric Froude number $v_s/[(\rho_s/\rho_f - 1)gd_p]^{0.5}$
Re_p	Particle Reynolds number $\rho_f v_s d_p/\mu$
Re_ε	Voidage Reynolds number $\rho_f v_s d_p/\mu(1\text{-}\varepsilon)$
Sc	Schmidt number ν_k/D_f
Sh	Sherwood number $(0.5Re_\varepsilon^{0.5} + 0.2Re_\varepsilon^{0.667})Sc^{0.333}$

1. Introduction

Water softening practices form an essential component in drinking water production, where drinking water production encompasses a series of treatment processes prior to distribution to consumers: Me-PO_4 coagulation and sedimentation, rapid sand filtration, ozonation, softening, biological active carbon filtration (BACF) and slow sand filtration. In this chain of treatment processes, drinking water softening significantly enhances public health, environmental conservation, social costs and client comfort by improving the hardness taste, odor and appearance of drinking water (Graveland et al., 1983; Van Ammers et al., 1986; Van Dijk and Wilms, 1991; Hofman et al., 2006). The softening process not only precipitates heavy metals due to induced alkaline conditions (Twort et al., 2000), but also plays a vital role in environmental conservation by reducing residues, such as phosphates, in drainage water. Additionally, it mitigates issues like clogging and limescale deposition in household and industrial water systems, thereby enhancing heating efficiency (Mitchell, 2008) and reducing the need of warm water equipment maintenance and washing powder usage (Hofman et al., 2006).

Nowadays, a worldwide annual drinking water volume of well over 35 billion cubic meters, which continues to grow, is softened by over 16,000 installed treatment plants (Eke et al., 2020), predominantly through three techniques: nanofiltration, ion exchange and seeded crystallization. In recent years, seeded crystallization through pellet-softening using fluidized bed reactors (FBRs) emerges as the prevalent softening method (Kramer, 2021). For instance, FBRs are recently being implemented on a large scale in Denmark (Tang, 2019) and are currently built in numerous countries across the globe, including Saudi-Arabia, South Africa and Australia (RoyalHaskoningDHV, 2024). In the Netherlands alone, an annual volume of almost 0.5 billion cubic meters of drinking water is softened by seeded crystallization (Kramer, 2021).

Pellet softening utilizes cylindrical FBRs filled with seeding material that is fluidized due to water upflow. For the removal of calcium, NaOH (caustic soda), $Ca(OH)_2$ (lime) or Na_2CO_3 (soda ash) is dosed based on influent water alkalinity and the composition of hardness-causing ions (Hofman et al., 2006; Van der Bruggen et al., 2009). The addition of softening chemicals elevates pH, causing the solubility product of $CaCO_3$ (calcium carbonate) to be exceeded, ideally leading to $CaCO_3$

crystallization onto the fluidized pellets.

However, despite advances in pellet softening techniques and practices, significant challenges remain. Current models used to predict and optimize calcium removal via FBRs suffer from several critical shortcomings: (1) lack of an integral process approach, (2) failure to account for recent process modifications, (3) absence of coherent key performance indicators (KPIs) and (4) oversimplified mixing assumptions.

During pellet-water softening, a part of the precipitating $CaCO_3$ may also be formed spontaneously in the water phase, which will flush out and is transported in the water to subsequent downstream filtration processes, like BACF. Water flows downward in the BACF bed, and, ideally, only small organic compounds, broken down by ozonation, are filtered out by adsorption of those compounds onto the biologically active carbon grains. However, flushed out $CaCO_3$ particles from the softening pellet reactors, known as fines, lead to problematic consequences in downstream processes and, for example, accelerate the decrease in operational lifetime of the BACF bed (Fig. 1). In addition, the production of fines results in diminished efficiency of permanently encapsulating biomass within the calcite pellets (Hammes et al., 2011).

Substantial advancements have been made and key changes in pellet softening include the transition from (Australian) garnet sand to locally-sourced and re-used calcite pellets (see supplementary information (SI)-I for images of the calcite pellets) for calcium removal, reflecting a shift towards more sustainable practices and the circular economy (Palmen et al., 2014; Schetters et al., 2015; Tang et al., 2019; Micari et al., 2020). In addition, significant updates in the softening chemical dosing techniques and modifications in targeted total hardness levels post-softening have been observed (Sobhan, 2019). Recent research suggests that initial improvements in pellet softening models could be achieved using bi-linear hydraulics and mass transfer kinetics (Van den Hout, 2016; Chiou, 2018; Seepma, 2018). These efforts were further refined by Sobhan (2019) and Bögels (2019), defining four operationally different hydraulic and mass transfer kinetic zones relative to the fluidized bed height. Also, the influence of supersaturation and calcite pellet bed height on the $CaCO_3$ fines production from homogeneous nucleation was studied (Bastiaan, 2020), and a larger production rate was found at high supersaturation with respect to calcite, colder temperatures and in hydraulically more turbulent zones. However, due to the limited data set, no generic relationship was established. Despite these advancements, they are often not considered in existing current kinetic models (Rietveld, 2005; Van Schagen, 2009) and, therefore, the existing models are debatable for representing the complexities of industrial-scale processes.

One of the critical barriers to improving the softening process is the absence of coherent and standardized KPIs (Kramer, 2021). KPIs are essential for monitoring and optimizing critical aspects of the process, such as chemical dosing efficiency, calcium removal rates, and fines production. Without well-defined KPIs, it becomes difficult to compare performance across different water treatment plants or reactor setups, as existing kinetic models often vary due to localized conditions – such as specific reactor designs, water matrix variations, and measurement methods. This lack of standardized performance metrics hinders both process optimization and scalability. Lastly, challenges remain in the assumption of uniform mixing between softening chemicals, influent water and seed material within FBRs, leading to inaccurate predictions of calcium removal.

The general need to concurrently manage homogeneous and heterogeneous $CaCO_3$ removal, implement the aforementioned recent process changes, and address the lack of an integral approach, the absence of coherent KPIs, and the oversimplified mixing assumptions in current models, calls for a new holistic and flexible model approach to improve softening process efficiency, reactor design and decision-making (Rietveld, 2005). Therefore, we propose a new mechanistic and predictive model. This model is mechanistic, because it is rooted in existing fundamental principles of standard water treatment and very often applied techniques such as filtration, absorption, nucleation, crystallization and fluidization processes. In addition, it is predictive, because it is designed to predict (1) $CaCO_3$ removal rates in drinking water more accurately through pellet softening, (2) assess the carry-over of produced $CaCO_3$ fines during pellet softening leaving the FBR, and (3) determine the saturation of the bed in the subsequent (i.e., downstream) treatment step of BACF. Our approach integrates insights from

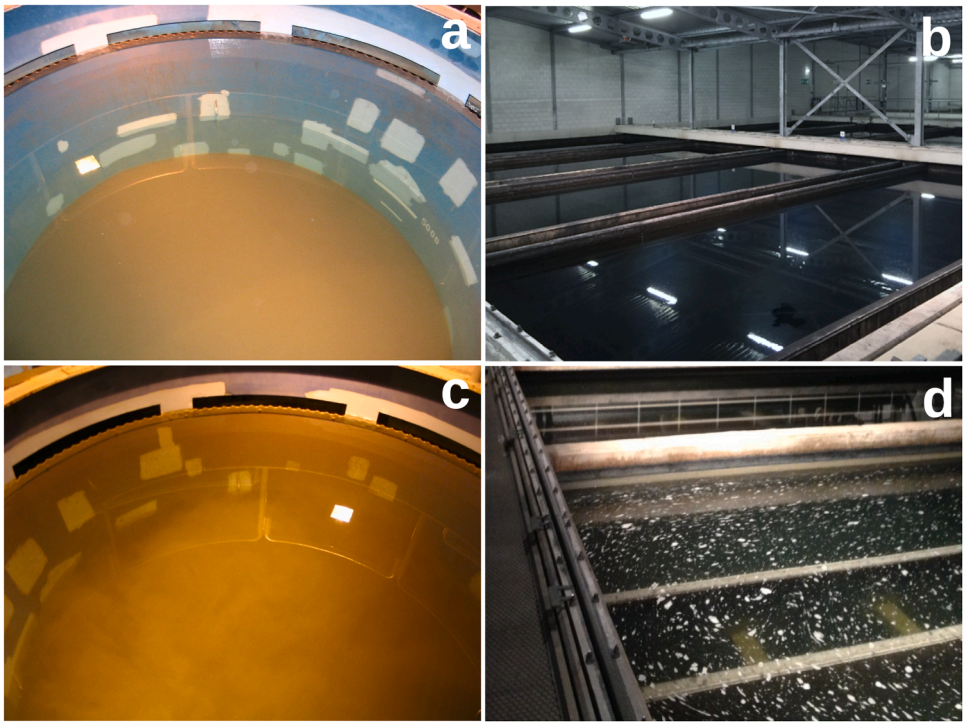

Fig. 1. Top of the softening fluidized bed reactor (a) and the downstream BACF bed (b) at optimal operational conditions, contrasted with the top of the softening fluidized bed reactor (c) and the BACF bed (d) at underperforming operational conditions with high amounts of fines.

hydrodynamic, thermodynamic, mass transfer kinetic, nucleation, and reactor engineering research fields, anchored on four critical independent variables: temperature (T), linear superficial velocity (v_s), pellet particle size diameter (d_p) and the saturation index with respect to $CaCO_3$ (calcite; SI_{cal}). These four variables overlap among the mentioned field disciplines, enabling the combination of research disciplines into one overarching model. To account for the degree of non-uniform mixing, SI_{cal}-values were varied over a broad range. Our innovative model provides predictions for KPIs in hydrodynamic, thermodynamic, mass transfer kinetic, crystallization and recrystallization efficiency, facilitating a deeper understanding of softening process performance, chemical usage, and reactor design. Our model was tested and validated by process and laboratory data on annual total calcite pellet removal and $CaCO_3$ fines production, as well as operator expertise from the Waternet Weesperkarspel drinking water treatment plant in Amsterdam, The Netherlands (WPK) and confirm the model's broad applicability beyond the initial testing site. Ultimately, this approach marks a significant step towards transforming drinking water treatment into a more circular and environmentally sustainable process.

2. Materials & methods

In this section, we present the methodology used to develop and validate the mechanistic model. Our approach encompasses theoretical foundations, data collection and model validation to ensure the stability and responsiveness of the model to variations in input parameters. While the general description of the model is presented here, the detailed step-by-step description is found in SI-II to SI-VII.

2.1. Heterogeneous crystallization

To describe the heterogeneous $CaCO_3$ crystallization rate during pellet-based softening, we used the following improved overarching relationship, which is based on Wiechers et al. (1975) and Van Schagen et al. (2008a):

$$J_c = \frac{\Delta m_{CaCO_3}}{A_r h_r M_W \Delta t_r} = K_c\ SSA_W \sqrt{\{Ca^{2+}\}\{CO_3^{2-}\} - K_{sp,\ calcite}} = K_c\ SSA_W\ CCPP \quad (1)$$

where J_c is the heterogeneous $CaCO_3$ crystallization rate [mol m^{-3} s^{-1}], m_{CaCO_3} is the mass lost due to crystallization [kg], A_r is the reactor area perpendicular to the fluid flow [m^2], h_r is the height of the pellet reactor in which $CaCO_3$ is able to crystallize [m], M_W is the molecular weight of $CaCO_3$ [kg mol^{-1}], t_r is the reaction time [s], K_c is the mass transfer coefficient [m s^{-1}], SSA_W is the specific surface area per water volume [m^2 m^{-3}] (i.e., the volume not occupied by solid particles), $\{Ca^{2+}\}$ and $\{CO_3^{2-}\}$ are the activities for the calcium and carbonate free ions in solution [mol m^{-3}] and $K_{sp,\ calcite}$ is the solubility product of calcite [mol^2 m^{-6}]. Note that the reaction time t_r in Eq. (1) represents the total duration of crystallization occurring within the FBR, which should ideally be less than the water residence time (i.e., $t_r < \tau_r$).

2.2. Homogeneous nucleation

Eq. (1) does not include the contribution of spontaneous homogeneous nucleation of $CaCO_3$ nuclei that ultimately form larger $CaCO_3$ particles in the water phase. Therefore, Eq. (1) was extended with an additional term that describes the nucleation rate. While there are various ways to quantify the nucleation rate of $CaCO_3$, we selected the expression based on single $CaCO_3$ ion pair formation (Verdoes et al., 1992):

$$J_p = J_c + J_n = \left[\frac{\Delta m_{CaCO_3}}{A_r h_r M_W \Delta t_r}\right]_c + \left[\frac{\Delta m_{CaCO_3}}{A_r h_r M_W \Delta t_r}\right]_n = K_c\ SSA_W\ CCPP + K_n \frac{V_c}{V_m} \sqrt{\frac{10^{SI_{cal}}\ 10^{K_{sp,\ vaterite}}}{10^{K_{sp,\ calcite}}}} \exp\left[\frac{-B_n}{ln\left[\sqrt{\frac{10^{SI_{cal}}\ 10^{K_{sp,\ vaterite}}}{10^{K_{sp,\ calcite}}}}\right]^2}\right] \quad (2)$$

where J_n is the $CaCO_3$ nucleation rate [mol m^{-3} s^{-1}], K_n is the nucleation rate constant [m^{-3} s^{-1}], V_c is the volume of a single $CaCO_3$ cluster [m^3], V_m is the molar volume of $CaCO_3$, $K_{sp,\ vaterite}$ is the solubility product of vaterite [mol^2 m^{-6}], SI_{cal} is the saturation index with respect to calcite [-] and B_n is the kinetic nucleation barrier constant [-] (De Yoreo and Vekilov, 2003).

2.3. Impact of $CaCO_3$ fines production on downstream treatment

Eq. (2) does not delineate the influence of $CaCO_3$ removal via pellet softening on the subsequent treatment step. To include that, differences in reactor dimensions, downstream bed characteristics and the volume expansion of the particulate material (i.e., $CaCO_3$ fines) compared to the ion pair have to be considered. Our emphasis was directed towards formulating a model to elucidate the impact on BACF (Van der Hoek et al., 1999; Bandosz, 2006; Crittenden et al., 2012), presuming it to be the subsequent treatment step. With the BACF bed height saturation velocity rate $r_{BACF}^{CaCO_3}$, we established a new relation between the nucleation rate J_n and the eventual impact on BACF (Eq. (3)):

$$r_{BACF}^{CaCO_3} = f(v_s,\ h_r)\ J_n \frac{M_W\ \varepsilon_{BACF}\ \frac{A_r}{A_{BACF}}}{\rho^{fines}} = f(v_s,\ h_r)\ K_n \frac{V_c}{V_m} \sqrt{\frac{10^{SI_{cal}}\ 10^{K_{sp,\ vaterite}}}{10^{K_{sp,\ calcite}}}} \exp\left[\frac{-B_n}{ln\left[\sqrt{\frac{10^{SI_{cal}}\ 10^{K_{sp,\ vaterite}}}{10^{K_{sp,\ calcite}}}}\right]^2}\right] \frac{M_W\ \varepsilon_{BACF}\ \frac{A_r}{A_{BACF}}}{\rho^{fines}} \quad (3)$$

where $f(v_s,\ h_r)$ is the recrystallization factor [-], ε_{BACF} is the average voidage of the BACF bed [-], A_{BACF} is the total cross-sectional area of BACF bed [m^2] and ρ^{fines} is the average density of the $CaCO_3$ fine particles formed by nucleation [kg m^{-3}]. Unlike pellet softening, the water flows downwards in BACF (i.e., it operates in fixed bed conditions) and therefore, the voidage of the BACF bed (ε_{BACF}) is constant and could explicitly be used in Eq. (3).

2.4. Integral model overview

To summarize, Eq. (1) contains considerations related to temperature, hydrodynamics, thermodynamics and mass transfer kinetics concerning heterogeneous calcium removal. Subsequently, Eq. (2) further refines the model and incorporates a nucleation factor to account for additional $CaCO_3$ removal by homogeneous nucleation. To enhance global optimization within the total drinking water treatment chain and to serve as a validation method, Eq. (3) introduces a downstream consequential factor: the BACF bed height saturation velocity rate. Eqs. (2) and (3) describe our mechanistic model and the relations are visually summarized in Fig. 2. It illustrates the comprehensive integration of temperature relations (in green), hydrodynamics (in red), thermodynamics (in yellow), mass transfer kinetics (in blue), nucleation (in purple) and the BACF component (in orange) into our model, aiming to

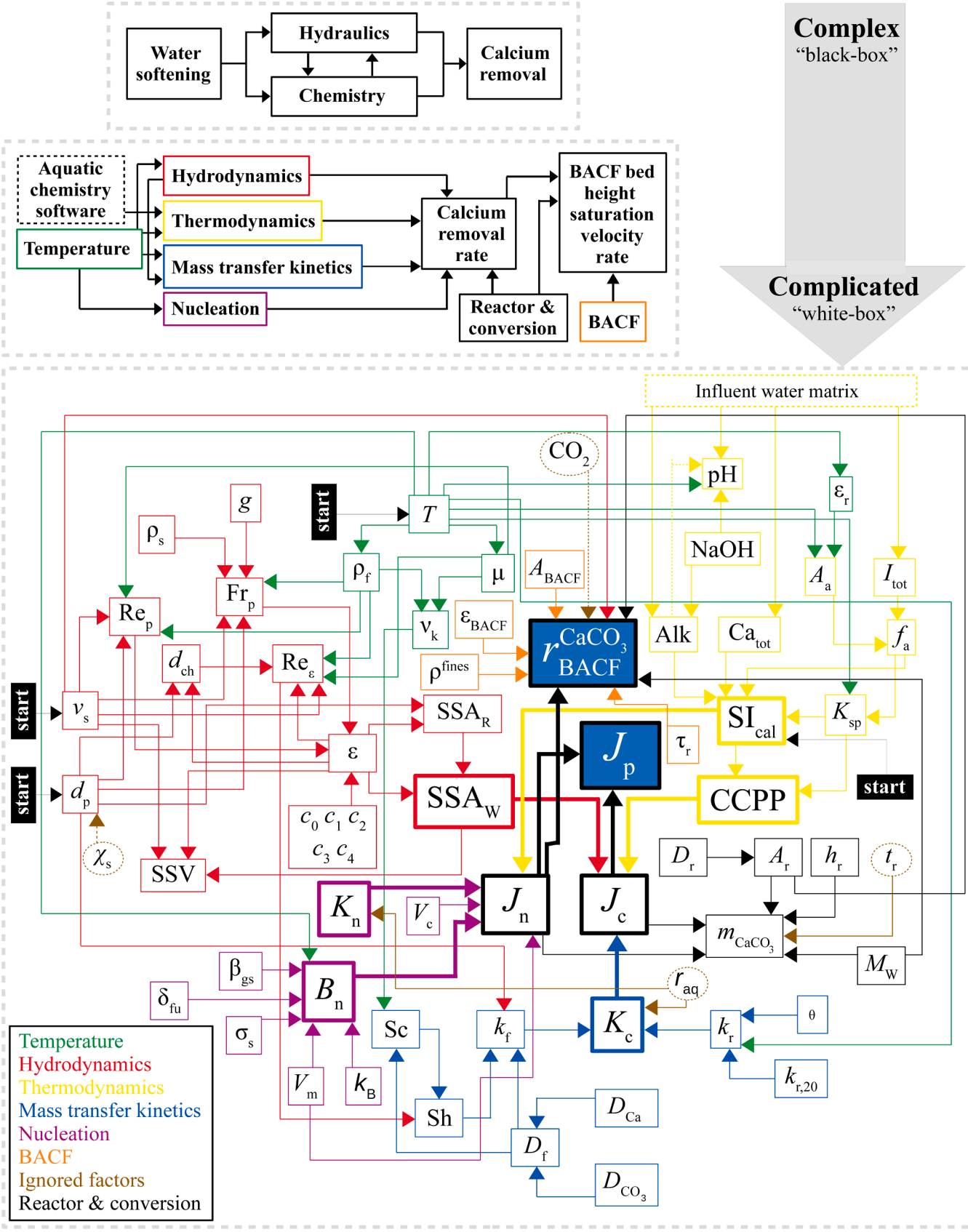

(caption on next page)

Fig. 2. Conundrum of the mechanistic model as presented in Eqs. (2) and (3). Three hierarchical levels of the proposed pellet-water softening model are illustrated, where model complexity decreases and model complicatedness increases from top to bottom. Therefore, this model transitions from an abstract "black-box" representation to a more transparent "white-box" model. Each color represents a different research discipline, with each color containing multiple parameters. The parameters within thicker-lined squares are directly shown in Eq. (3). The letters and symbols included are: In green – T (temperature), ρ_f (fluid density), μ (dynamic viscosity), ν_k (kinematic viscosity), ε_r (dielectric constant); In red – g (gravitational constant), ρ_s (calcite pellet density), Re_p (particle Reynolds number), Fr_p (densimetric Froude number), v_s (linear superficial fluid velocity), d_p (particle size diameter), ε (voidage of the fluidized pellet bed), c_0-c_4 (fit coefficients belonging to the Rep2Frp model; Kramer et al. (2020)), d_{ch} (channel diameter), Re_ε (voidage Reynolds number), SSA_R (specific surface area in empty reactor volume), SSA_W (specific surface area in water volume), SSV (specific space velocity); In yellow – influent water matrix (i.e., characteristics of solutes and their concentration), pH (pH of the water matrix), NaOH (concentration dosage of NaOH), Alk (alkalinity), A_a (activity prefactor), I_{tot} (total ionic strength of the water matrix), f_a (activity coefficient of specific ions), K_{sp} (solubility product of calcite), SI_{cal} (saturation index with respect to calcite), CCPP (theoretical calcium carbonate precipitation potential); In blue – θ (reaction order constant), $k_{r,20}$ (reference reaction order at 20 °C), k_r (surface reaction rate coefficient), k_f (diffusional mass transfer coefficient), K_c (crystallization rate constant), Sc (Schmidt number), Sh (Sherwood number), D_f (ion pair diffusion coefficient), D_{Ca} and D_{CO_3} (diffusion coefficient of respectively Ca and CO_3); In purple – δ_{fu} (number of formula units), β_{gs} (geometric shape factor), σ_s (specific surface free energy), V_c (cluster volume), V_m (molar volume), k_B (Boltzmann constant), B_n (nucleation barrier constant), K_n (nucleation rate constant); In orange – ρ^{fines} (density of carry-over particles), ε_{BACF} (fixed bed voidage of BACF), A_{BACF} (total cross-sectional area of the BACF bed), τ_r (average water residence time); In black – D_r (pellet reactor diameter), A_r (pellet reactor cross-sectional area), h_r (pellet reactor height), m_{CaCO_3} ($CaCO_3$ mass), M_W (molecular weight), J_n, J_c and J_p (molar nucleation, crystallization and precipitation rate) and $r_{BACF}^{CaCO_3}$ (BACF bed height saturation velocity rate due to $CaCO_3$ carry-over). In brown, parameters t_r (reaction time), χ_s (particle shape factor), r_{aq} (solution stoichiometry) and CO_2 (i.e., CO_2 dosing after drinking water softening, but before BACF) are shown, which were not included in our model. The starting point in the most complicated model is at one of the four independent parameters (indicated by "start") and ultimately ends at the output model variables of J_p and $r_{BACF}^{CaCO_3}$.

provide a holistic understanding of the water softening process practiced by pellet bed fluidization and allowing for a more accurate and predictive model.

3. Results & discussion

In Sections 3.1 and 3.2, we elucidate our findings for the modeled resultants J_p and $r_{BACF}^{CaCO_3}$ at $T = 12$ °C, which is the average water temperature at WPK (Figure S6 in SI-VIII). However, the intermediate modeling results, showing how the variables ρ_f, μ, ν_k, ε_r, Re_p, Re_ε, Fr_p, ε, SSA_R, SSA_W, SSV, CCPP, k_r, Sh, J_p and $r_{BACF}^{CaCO_3}$ depend on all their respective independent variables, are found as Figures S7-S36 and discussed in SI-IX and SI-X (see nomenclature for the meaning of each parameter). In our modeling effort, d_p was constrained to a range of 0.5 to 3.5 mm and v_s to 50 – 150 m/h. These ranges were selected, because they cover a wide array of process conditions commonly encountered in industrial settings and especially in drinking water treatment processes that make use of FBRs (Graveland et al., 1983; Van Dijk and Wilms, 1991; Aldaco et al., 2008; Van Houwelingen et al., 2010; Hu et al., 2017). Nevertheless, we also used our model to explore conditions beyond these specified ranges, in terms of ε and SSV, and the corresponding results (i.e., Figures S36 and S37) and discussion are found in SI-XI. To provide context to our modeling results, we defined a model range of process conditions for research purposes, a softening range for engineering improvement opportunities and average WPK process conditions for validation purposes (SI-XII). In Section 3.3, the approach on the model validation is discussed and in Section 3.4, the five proposed KPIs, SSV, $CCPP_{rel}$, Sh, J_c / J_p and $f(v_s, h_r = 4.5\text{ m})$, crucial to pellet softening are evaluated. Thereafter, reactor process conditions recommendations, to improve calcium removal by crystallization and to prevent downstream BACF clogging, are proposed in Section 3.5, followed by the uncertainty discussion (Section 3.6), model limitations (Section 3.7) and implications (Section 3.8).

3.1. Total calcium removal rate model predictions

The first of two overarching results of the model is the total calcium removal rate in a fluidized bed setting: J_p. Fig. 3 shows J_p at $T = 0$, 20 and 40 °C (columns) and at $d_p = 0.5$, 1.1 and 3.5 mm (rows). Note that Fig. 3 only shows J_p for $SI_{cal} = 0 - 3$ to highlight the transition of a heterogeneous crystallization dominated system to a homogeneous nucleation dominated system (Figure S25d), while Figures S26-S30 in SI-X show J_p for $SI_{cal} = 0 - 5$ and $T = 0$, 10, 20, 30 and 40 °C.

Expectedly, J_p generally increases with increasing T (i.e., Fig. 3a, d and g versus Fig. 3b, c, e, f, h and i). However, at low J_p, this trend seems slightly reversed, and is best observed when the most left contour line in Fig. 3d is compared to 3e and 3f. The point of reversal in this behaviour lies somewhere between 0.001 – 0.01 mol m^{-3} s^{-1}. In addition, at small d_p, a significantly larger calcium removal rate is observed compared to larger d_p for $SI_{cal} \leq 2.5$ (i.e., Fig. 3a versus d and g, 3b versus e and h and 3c versus f and i). For example, at $SI_{cal} = 2.0$ and $T = 20$ °C, this effect results in a 2.5 times larger rate at $d_p = 0.5$ mm compared to $d_p = 1.1$ mm (i.e., ~ 0.45 versus 0.20 mol m^{-3} s^{-1} respectively). However at $SI_{cal} > 2.5$, this trend becomes increasingly less significant. Furthermore, at lower values of J_p, a change in v_s has a larger impact on a relative change in J_p, which is best observed when Fig. 3g is compared to 3a.

In summary, water softening in terms of total calcium removal is locally optimized by maintaining small d_p, high v_s and high initial SI_{cal} and, if possible, at higher T. However, for a global optimization in the chain of drinking water treatment processes, the consequences of the selected process conditions for the next step in water treatment should be evaluated.

3.2. Model predictions of bed clogging in subsequent treatment process

Fines formed in the FBR that do not attach and recrystallize inside the FBR are transported to the next treatment step, such as BACF. The $r_{BACF}^{CaCO_3}$ describes the rate at which the BACF bed can become saturated with fines and Fig. 4 shows the $r_{BACF}^{CaCO_3}$ versus v_s and SI_{cal} at $T = 12$ °C, while Figure S36 in SI-X shows the influence of T. As long as $SI_{cal} < 1.8$, there is an insignificant build up of BACF bed saturation by $CaCO_3$. At $SI_{cal} \sim 2.0$, $CaCO_3$ causes a $r_{BACF}^{CaCO_3}$ of approximately 0.01 - 0.1 mm $month^{-1}$ s^{-1} according to our model. Note that at $SI_{cal} \leq 2.0$, the BACF bed saturation build-up is nearly independent of v_s, while at $SI_{cal} > 2.0$, it becomes increasingly more dependent on v_s, where an increase in v_s leads to a faster $r_{BACF}^{CaCO_3}$. To convert $r_{BACF}^{CaCO_3}$ into $v_{BACF}^{CaCO_3}$, the total reaction time t_r for J_n is required. The difficulty is that t_r is not constant and varies with T and SI_{cal}. For average WPK conditions, we estimated $t_r \sim 16$ s (SI-XIII), resulting in $v_{BACF}^{CaCO_3} \sim 0.39$ mm $month^{-1}$.

3.3. Model validation

In this work we propose a novel mechanistic model, making it crucial to validate its quality. The model's validation was conducted with long-term data on annual calcite pellet mass removal at the WPK plant and with laboratory particle count and size measurements to estimate BACF bed clogging, complemented by operators' estimations on $CaCO_3$ fines removal from piping leading to BACF and the top of the BACF beds at WPK. Detailed validation procedures and results are discussed in SI-XIII and SI-XIV, which generally support the model's predictions, indicating

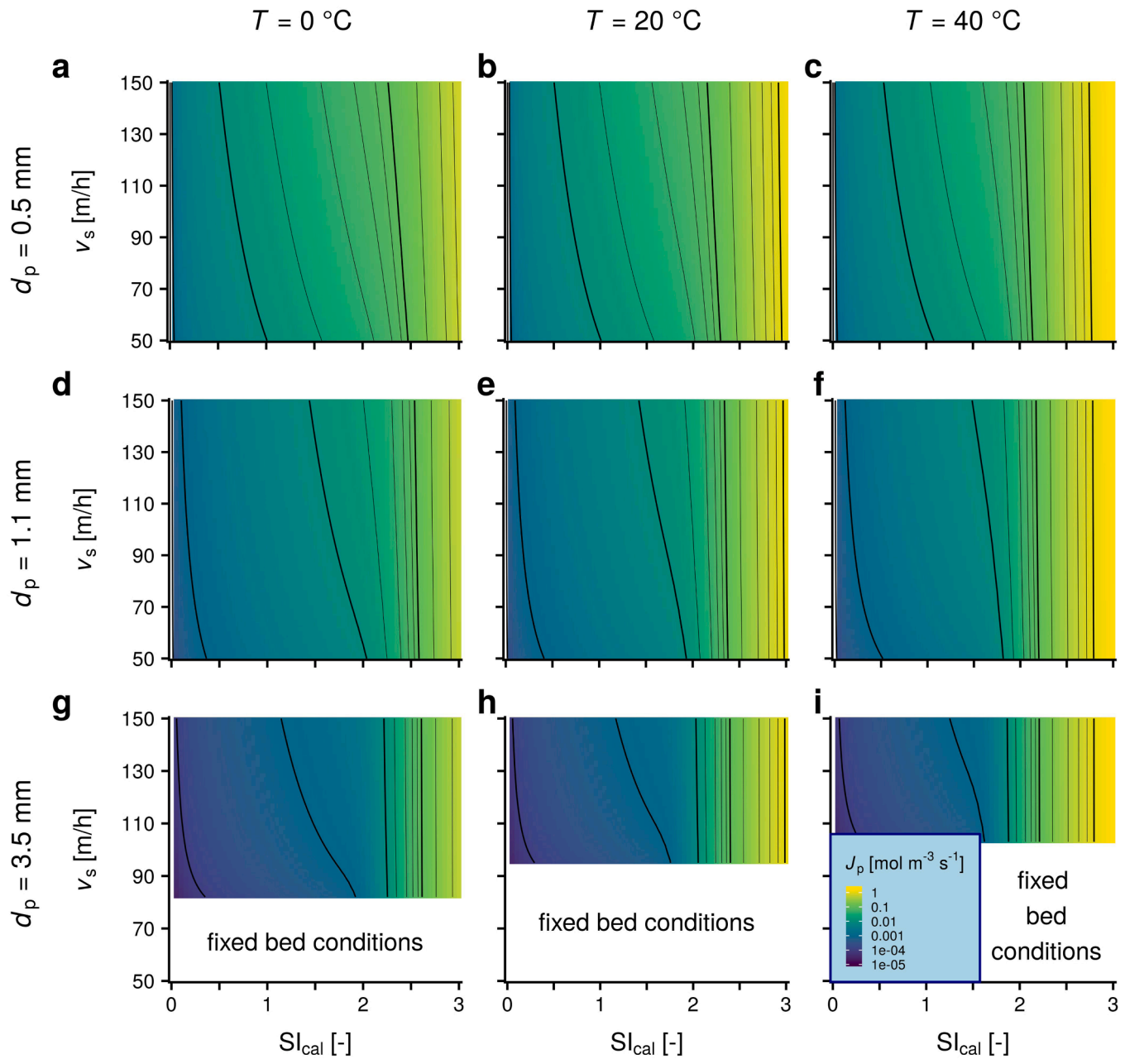

Fig. 3. Total $CaCO_3$ precipitation rate (J_p) versus linear superficial velocity (v_s) and calcite saturation index (SI_{cal}) for temperature (T) = 0, 20 and 40 °C (i.e., the column variable) and d_p = 0.5, 1.1 and 3.5 mm (i.e., the row variable); J_p for d_p = 0.5 mm and T = 0 °C (a), d_p = 0.5 mm and T = 20 °C (b), d_p = 0.5 mm and T = 40 °C (c), d_p = 1.1 mm and T = 0 °C (d), d_p = 1.1 mm and T = 20 °C (e), d_p = 1.1 mm and T = 40 °C (f), d_p = 3.5 mm and T = 0 °C (g), d_p = 3.5 mm and T = 20 °C (h) and d_p = 3.5 mm and T = 40 °C (i). The logarithmic color scale is the same for each figure and is blue at 0.00001 and yellow at > 1 mol m^{-3} s^{-1}. The black contour lines are a guide to the eye and the thicker ones are marked at each order of magnitude with base 10, while the thinner ones are placed at 0.02, 0.04, 0.06, 0.08, 0.2, 0.4, 0.6 and 0.8, respectively. Note that at low v_s for d_p = 3.5 mm (i.e., g-i), undesirable fixed bed conditions apply. Simulated data of J_p at other d_p-values and at T-values are found as Figures S26-S30 in SI-X.

reliability and applicability.

3.4. Key reactor performance indicators

Our model encompasses five key reactor performance indicators to optimize pellet softening locally (Fig. 5). Firstly, the SSV evaluates the hydrodynamic conditions, optimal within v_s = 50 – 150 m/h and d_p = 1.0 – 3.5 mm, but is significantly reduced at d_p < 1.0 mm, especially at T ≤ 5 °C (Figure S16). Secondly, thermodynamic conditions are assessed by $CCPP_{rel}$, notably effected by T < 5 °C, demanding increased NaOH dosing for 99 % efficiency. Thirdly, crystallization efficiency, evaluated by the J_c / J_p ratio, shifts from heterogeneous crystallization to undesirable homogeneous nucleation between SI_{cal} = 2 – 3. However, at high T (i.e., T > 35 °C), undesirable homogeneous nucleation becomes more dominant at SI_{cal} ~ 1.8. Fourthly, Sh assesses the mass transfer kinetics and a high Sh is most favorable for convective-driven mass transfer. Sh becomes critically problematic near fixed bed conditions, but d_p ≤ 1.0 mm also leads to unstable conditions due to increased bed heterogeneity. Fifthly, the recrystallization efficiency, dependent on the water residence time (τ_r), is effective at τ_r ≥ 5 min, displays room for improvement at 5 min < τ_r < 3 min and declines sharply at τ_r < 3 min. At τ_r < 3 min, it negatively affects downstream $CaCO_3$ fines transport.

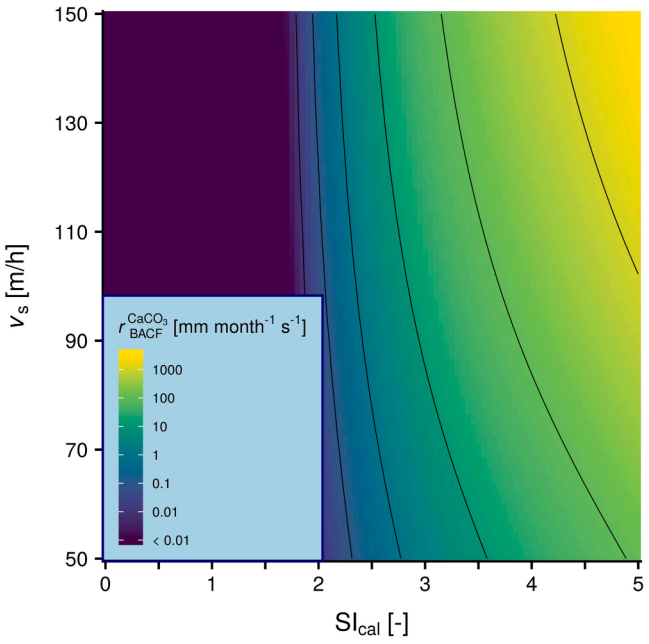

Fig. 4. $r^{CaCO_3}_{BACF}$ versus v_s and SI_{cal}. The black contour lines are a guide for the eye and are drawn at every order of magnitude between 0.01 – 1000 mm month^{-1} s^{-1}. Simulated data of $r^{CaCO_3}_{BACF}$ at other T-values is found as Figure S36 in SI-X.

These KPIs facilitate the evaluation of pellet water softening performance with implications for local improvement and implementation and a more detailed elaboration is found in SI-XV.

3.5. *Reactor process condition recommendations for robust and flexible pellet water softening practices*

Our goal of achieving an integral optimization throughout the water treatment process, including ozonation, softening, and BACF, is reflected in recommendations derived from our model and focus on process condition optimization for pellet water softening with FBRs, particularly those that make use of dosing nozzles at the bottom of the reactor for mixing of softening chemicals with influent hard water. Fig. 6 shows the recommended v_s at $T = 12$ °C and varying d_p, with FBRs of certain height. The v_s recommendations depend on the aimed $CaCO_3$ recrystallization efficiency and Fig. 6a and 6b show respectively the scenarios targeting 90 % and 95 %. In addition, Figure S43 and S44 in SI-XVI show the recommendations for those scenarios at $T = 0 - 44$ °C. Minimal fluidization conditions were considered and is evident in Fig. 6a and 6b by the white areas at large d_p. Interestingly, at average WPK process conditions (i.e., $v_s \sim 80$ m/h), the minimal fluidized bed height in the FBR should be approximately 4.5 meter to maintain 90 % recrystallization efficiency. A lower v_s of 55 m/h is recommended to increase the recrystallization efficiency to 95 %, such that less $CaCO_3$ fines end up in the BACF bed. Alternatively, if $v_s = 80$ m/h is preferred, FBRs should be constructed with a minimum height of 6.5 m rather than 4.5 m to reach 95 % recrystallization efficiency.

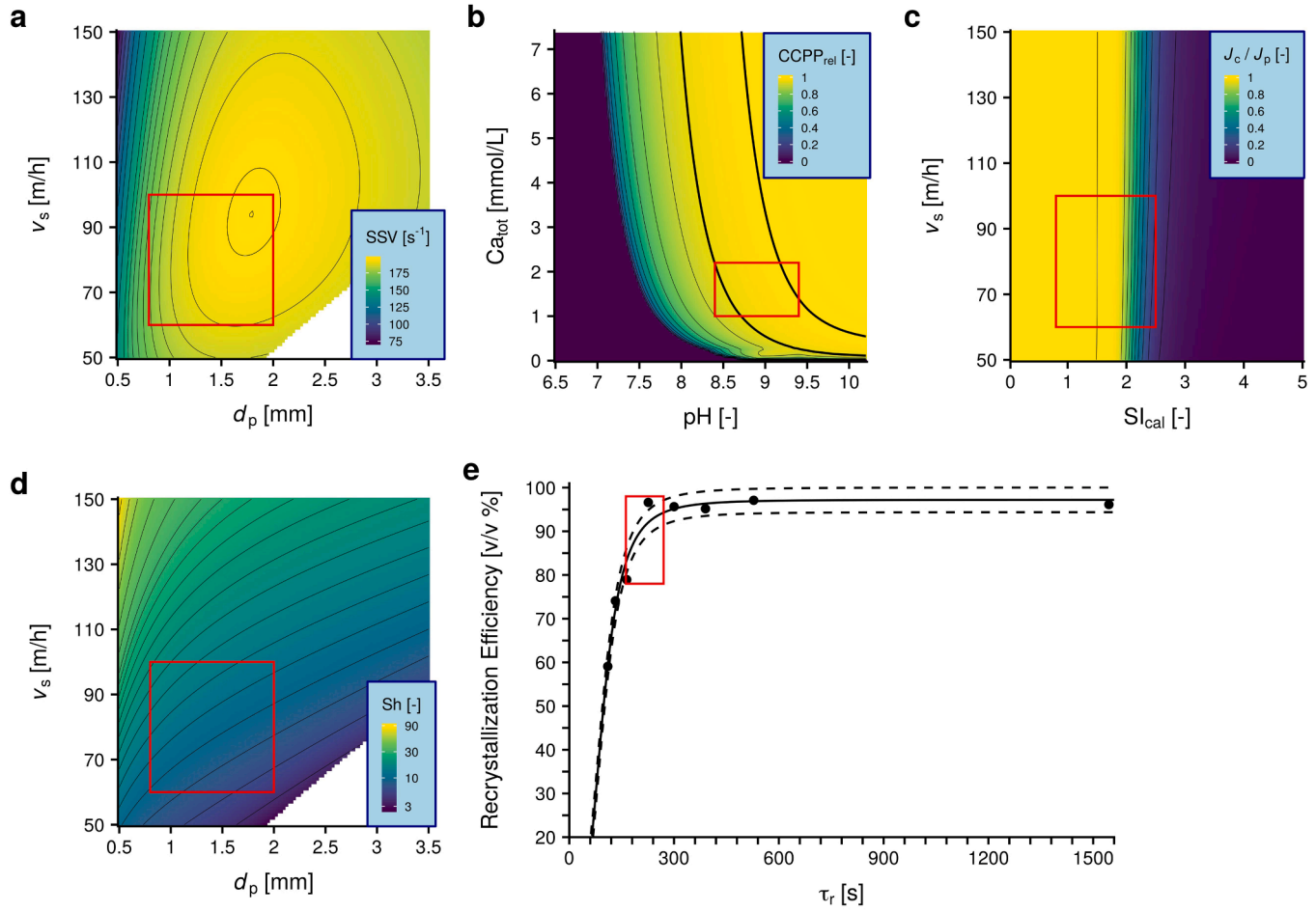

Fig. 5. KPI evaluation of the hydrodynamic SSV (a), thermodynamic $CCPP_{rel}$ (b), mass transfer kinetic Sh (c), crystallization efficiency (d) and recrystallization efficiency (e). The red marked areas represent the commonly encountered process conditions during pellet softening. The yellow areas in (a-d) are the most optimal conditions and when τ_r increases toward 10 min (e). However, improving one KPI may lead to worsening another KPI.

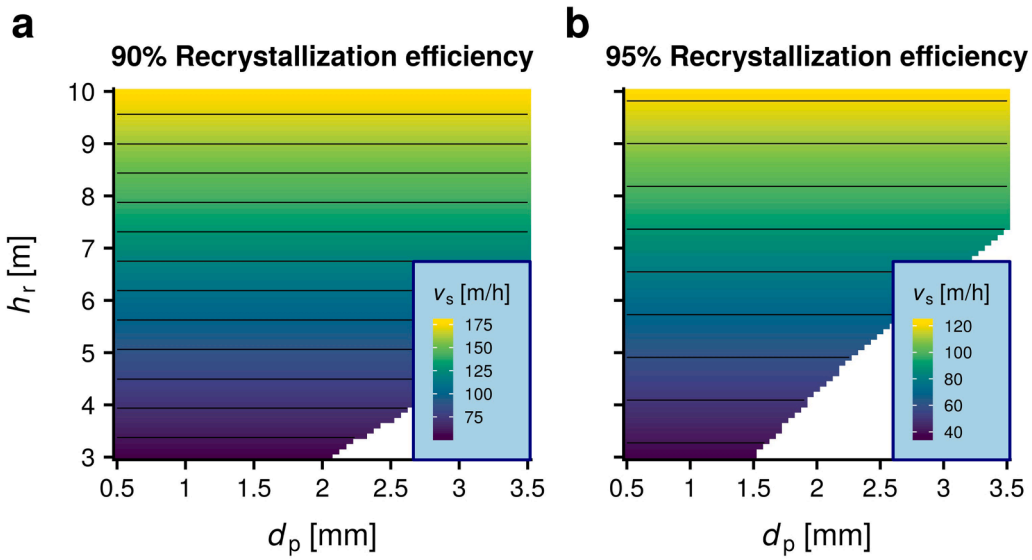

Fig. 6. Reactor process conditions recommendations in terms of v_s versus reactor height (h_r) and particle size diameter (d_p). The black contour lines are a guide to the eye and are marked every 1 m. Note that at large d_p and low v_s, fixed bed conditions apply.

3.6. Uncertainties of the model

First of all, our model is improved by integrating the latest voidage (ε) prediction model (Kramer et al., 2020). Unlike previous models that relied on numerical methods (Carman, 1937; Ergun, 1952; Richardson and Zaki, 1954; Wen and Yu, 1966; Foscolo et al., 1983; Van Dijk and Wilms, 1991; Di Felice, 1995; Akgiray and Soyer, 2006; Van Schagen et al., 2008b), this voidage prediction model significantly improves the accuracy by accounting for heterogeneity within the fluidized bed. Whereas the prediction error of past models is at best about 5 %, our model prediction error for ε is approximately 1.9 % (Kramer et al., 2020). Secondly, we separated the thermodynamic part of the calculations from our model, because different thermodynamic databases calculate slightly different values for SI_{cal}. We compared the calculated SI_{cal} for the llnl, wateqv4, phreeqc and minteqv4 databases and they vary up to about 1 % at most (Figure S45 in SI-XVII). In addition, our study focused on water softening through NaOH dosing and, therefore, our thermodynamic calculations were performed with NaOH addition. However, because our thermodynamic calculations are separated from the model, NaOH can be replaced by $Ca(OH)_2$ or Na_2CO_3 in new thermodynamic calculations for SI_{cal}. Thirdly, the largest uncertainties within our model likely reside in K_n, σ_s, Sh and $f(v_s, h_r = 4.5\ m)$, where K_n has by far the largest absolute uncertainty. By fitting to fluidized bed experimental data of Mahasti et al. (2017), we obtained a value for K_n which is roughly a million times larger than the value found by Verdoes et al. (1992) with thermostat batch reactor experiments. While, this difference seems large, it makes sense that more nuclei form in a more turbulent and heterogeneous flow regime. Besides, our K_n is still 7 – 13 orders of magnitude lower than a purely homogeneous nucleation regime. Similarly, σ_s in our model is close to the value suggested by Verdoes et al. (1992) (SI-II.5.). Fourthly, many different expressions for the Sh number exist, derived from numerous data sets (e.g., Kunii and Levenspiel, 1969; Whitaker, 1972; Upadhyay and Tripathy, 1975; Tournie et al., 1977, 1979; Gunn, 1978; Ballesteros et al., 1982; Arters and Fan, 1986; Bošković et al., 1994; Tai et al., 1999; Bošković-Vragolović et al., 2007; Derksen, 2014; Kalaga et al., 2014), each defined by specific boundary conditions on fluid characteristics and particle properties. We chose for the expression derived by Whitaker (1972), because it is based on differently shaped particles (i.e., cubes and spheres), as well as a wide range in bed voidage (i.e., $\varepsilon = 0.34 - 0.78$) and Reynolds number (i.e., $\sim 10 < Re_\varepsilon < 10^4$). Whitaker (1972) estimated that, despite the large range in Re_ε, ε and χ_s, all of the predicted Sh-values by Equation S27 in SI-II.4 lie within 25 % (i.e., ~ 3 SD). Fifthly, our fitting of the recrystallization factor $f(v_s, h_r = 4.5\ m)$ has a relative SD of 2.8 % (Fig. 5e). However, it should be mentioned that $f(v_s, h_r = 4.5\ m)$ is significantly influenced by various factors, including reactor dimensions, type and concentration of softening chemicals used for mixing with influent hard water and maintenance condition of the FBR. Over time, partial clogging of mixing devices such as pumps, valves and dosing nozzles can occur, further impacting $f(v_s)$. The relation of v_s on $f(v_s)$ was largely based on the experimental data of Mahasti et al. (2017) on mass transfer, nucleation and recrystallization behaviour in a FBR setting, showing the effect of varying molar ratio (i.e., $r_{aq} = \{Ca^{2+}\}:\{CO_3^{2-}\}$), initial SI_{cal} and τ_r on nucleated versus crystallized $CaCO_3$ mass. Though, the fluidized bed $CaCO_3$ nucleation and crystallization studies of Sioson et al. (2019) and Tiangco et al. (2019) generally supported the findings of Mahasti et al. (2017), they did not investigate all of the aforementioned effects and had less experimental data at hand. In summary, while the mechanistic principles underlying the recrystallization efficiency are likely adequate, uncertainties persist regarding the variability of $f(v_s)$ across differently operated FBRs, dosing and mixing techniques and different maintenance levels.

With all the aforementioned uncertainties taken into account, the propagation error of our model for J_p and $r_{BACF}^{CaCO_3}$ was investigated thoroughly (SI-XVII) and shows that for both resultants, the propagation error is not constant and depends on the values for d_p, v_s, SI_{cal} and T as well as the degree of mixing $(\sigma_{SI_{cal}})$. We estimated that J_p and $r_{BACF}^{CaCO_3}$ have an average relative SD of respectively 40 % and 130 %.

3.7. Model evaluation and future considerations

Firstly, our model does not take into account particle shape or a shape factor (i.e., χ_s, Fig. 1). Calcite pellets come in all shapes (Kramer, 2021) and the shape factor likely influences d_p. When improvements of our model were to be made by means of χ_s, then it should be included as a factor to d_p, just as we presented in Fig. 2. Circularity, solidity, roundness or sphericity shape descriptors to represent χ_s may be useful to implement. Secondly, our model does not include any processes that are conducted between water softening in FBRs and BACF. One of such practices is CO_2 dosage (Fig. 2) to limit $CaCO_3$ precipitation after the water softening process. However, after softening, SI_{cal} is often near or well within the metastable zone ($-0.25 < SI_{cal} < 0.25$) and therefore the effect of CO_2 dosing is likely less significant on $v_{BACF}^{CaCO_3}$. Thirdly, we did

not implement or account for solution stoichiometry in our model. Solution stoichiometry (i.e., $r_{aq} = \{Ca^{2+}\}:\{CO_3^{2-}\}$) is known to have a significant effect on $CaCO_3$ formation and its formation is significantly slowed down at more extreme ratios, especially at $r_{aq} < 0.01$ and $r_{aq} > 100$ (Nehrke, 2007; Stack and Grantham, 2010; Sand et al., 2016; Seepma et al., 2021). r_{aq} directly effects both K_n and K_c (Fig. 2). During softening, r_{aq} varies from about 2 at the point of (homogeneous) mixing to 50 after softening for an average water composition (Table S2) at initial $SI_{cal} \sim 2.0$ and $T = 12$ °C. Therefore, extreme ratios are likely avoided and we don't expect a dominant effect in J_p by r_{aq}. Fourthly, inhibitory kinetic effects by other ions present in the water matrix (Sobhan, 2019; Chiou, 2018; Seepma, 2018) have not been included, as it would significantly reduce the universal applicability of our model. Inhibitory kinetic effects could be included into the model similarly to r_{aq}, as they would lower K_n and K_c by a quantifiable percentage. Lastly, while Eq. (2) would suit any type of FBR, Eq. (3) (i.e., the validation step with $r_{BACF}^{CaCO_3}$) was specifically validated for cylindrical FBRs with dosing nozzles at the bottom of the reactor. Especially, small changes in SI_{cal} have already a relatively significant impact on J_n and $v_{BACF}^{CaCO_3}$ (Sections 3.1 and 3.2). Therefore, other types of FBRs, for example conical ones, and/or with different mixing techniques between softening chemicals and influent hard water, might lead to a larger discrepancy between predicted values by our model and real-time measured data as well as the prediction error.

3.8. Implications

Our work implies that mixing of softening chemicals and influent hard water has a significant effect on the outcome of calcium removal rates and BACF bed height saturation velocity, due to a sharp non-linear increase at $SI_{cal} = 2 - 3$ (Fig. 4), as well as on the model's prediction error (Figure S46 and S47). Potentially, by insight and experience on the mixing behavior in the FBR through experimental data, our model framework may be adjusted accordingly to enhance current predictions and the associated prediction errors (Section 3.6). In SI-XVIII, we provide a detailed example demonstrating how the model equations can be applied using full-scale plant data, including a breakdown of variables that need to be measured, calculated, or sourced from the literature.

Generally, our model has shown that by combining different research disciplines, a more complete picture is provided on the mechanistic principles of water treatment, and in particular, water softening. In our mechanistic modeling, KPIs are retrieved to evaluate the system's hydrodynamic, thermodynamic, mass transfer kinetic, crystallization and recrystallization efficiency by means of respectively SSV, $CCPP_{rel}$, J_c / J_p, Sh and $f(v_s, h_r)$ (Section 3.4). Immediate measures for improving local pellet softening practices involve modifying the fluid properties, such as chemical dosing volume or concentration, water discharge, and water bypass, or changing the particle properties, such as the pellet particle size and fluidized bed height. Intermediate options for process improvement entail installation of alternative mixing devices or filters that capture $CaCO_3$ fines. If improvements cannot be made by the aforementioned strategies due to the current FBR dimensions or because v_s does not allow for further optimization, especially with regards to $f(v_s, h_r)$, then recirculation of the influent hard water may be a valuable option, resulting in a twofold increase of τ_r. Alternatively, more complex interventions such as energy-intensive temperature regulation methods may improve softening operations.

To practice water softening in a more flexible manner in terms of v_s (or aimed total water volume to-be-softened), future-build FBRs should have a minimum reactor height to allow for maximum recrystallization efficiency of homogeneously formed $CaCO_3$ fines. For example, when FBRs are build containing a 4 meter high bed, it allows for flexibility of v_s up to 50 m/h for a near maximum recrystallization efficiency of 95 %, while reactors of 6 m and 8 m bed allow for a flexible v_s up to 73 m/h and 97 m/h with the same efficiency. With increasing future water demands and the need of more water production and treatment expansion (H_2O waternetwerk, 2021), one should take into account the long-term needs as well as cost-benefit balance when building FBRs in relation to crystallization and chemical removal purposes.

Beyond water softening, our model serves as a versatile framework adaptable to a broad range of industries. By integration of fluid dynamics, particle growth, and chemical kinetics, it provides a solid foundation for applications in biological treatment and nutrient removal in wastewater treatment, chemical manufacturing, fermentation, crystallization in the food and beverage industry, pharmaceutical dissolution rate prediction, mining and mineral processing, and energy production. The model's wide applicability makes it a powerful tool for optimizing and enhancing processes across these diverse sectors.

4. Conclusions

Our new mechanistic model provides novel insights for enhancing the performance of pellet softening practices and identifies the specific areas of softening that may require optimization for maximum process improvement. Our model's key findings include:

- An integral plant-wide mechanistic approach is necessary that considers the impacts on and contributions of both upstream and downstream treatment processes for effective optimization.
- Identification of KPIs, such as SSV, $CCPP_{rel}$, J_c / J_p, Sh number and $f(v_s, h_r)$, for assessing the pellet softening performance, which reduce multiple dimensions and enables the transition from a black box to a more white box model.
- The observation that the downstream BACF bed experiences significant saturation over time when softening is practiced with initial $SI_{cal} > 2.0$ and that optimal process conditions for pellet softening by FBRs are highly dependent on water residence time, determining the recrystallization efficiency of $CaCO_3$ fines onto calcite pellets.

Funding

This work was supported by the European Research Council (ERC) under the European Union's Horizon 2020 Research and innovation programme (grant agreement no. 819588) to M.W., S.Y.M.H.S. and J.A.K.

Supplementary Information

Details are provided on images of calcite pellets (I), the equations and parameters used in the model (II), dependent-independent variable relations (III), $CaCO_3$ fines particle size (IV), fitting procedure of nucleation rate constant and specific surface free energy (V), relationship of recrystallization efficiency on water residence time and linear superficial velocity (VI), equations of all variables in terms of independent variables (VII), water temperature at Waternet Weesperkarspel (VIII), intermediate temperature, hydrodynamic, thermodynamic and kinetic mass transfer modeling results (IX), additional figures related to the results of the final modeling resultants (X), hydrodynamic behaviour beyond common process conditions (XI), definitions on the range of specific process condition values (XII), validation results and discussion of the mechanistic model (XIII and XIV), elaboration on key reactor performance indicators (XV), additional figures on reactor process conditions recommendations (XVI), relative propagation error calculations related to the model (XVI) and model implementation using treatment plant data (XVIII).

CRediT authorship contribution statement

Sergëj Y.M.H. Seepma: Writing – review & editing, Writing – original draft, Visualization, Validation, Software, Methodology, Investigation, Formal analysis, Data curation. **Janou A. Koskamp:**

Writing – review & editing, Software, Investigation, Formal analysis, Data curation, Conceptualization. **Michel G. Colin:** Writing – review & editing, Supervision, Resources, Project administration, Funding acquisition, Conceptualization. **Eleftheria Chiou:** Writing – review & editing, Methodology, Investigation, Conceptualization. **Rubayat Sobhan:** Writing – review & editing, Methodology, Investigation, Conceptualization. **Tim F.J. Bögels:** Writing – review & editing, Methodology, Investigation, Conceptualization. **Tom Bastiaan:** Writing – review & editing, Methodology, Investigation, Conceptualization. **Hadi Zamanian:** Writing – review & editing, Investigation, Data curation. **Eric T. Baars:** Writing – review & editing, Supervision, Methodology. **Peter J. de Moel:** Writing – review & editing, Supervision, Software, Methodology, Conceptualization. **Mariëtte Wolthers:** Writing – review & editing, Supervision, Resources, Project administration, Funding acquisition, Data curation, Conceptualization. **Onno J.I. Kramer:** Writing – review & editing, Supervision, Software, Resources, Project administration, Methodology, Data curation, Conceptualization.

Declaration of competing interest

The authors declare that they have no known competing financial interests or personal relationships that could have appeared to influence the work reported in this paper.

Acknowledgements

The authors thank F. te Pas, M. Joosten, P. Wind, B. van der Sluijs for their contribution in the arrangement of materials and equipment in the Waternet Weesperkarspel pilot plant and L. Kors for the administrative arrangements of having access to the treatment plant facilities.

Supplementary materials

Supplementary material associated with this article can be found, in the online version, at doi:10.1016/j.watres.2024.122781.

Data availability

The Excelsheet and mathematica file for calculations of respectively prediction rates and relative error percentage can be found as supplementary information files.

References

Akgiray, O., Soyer, E., 2006. An evaluation of expansion equations for fluidized solid-liquid systems. J. Water Supply Res. Technol. AQUA, 55 (7–8), 517–526. https://doi.org/10.2166/aqua.2006.040.

Aldaco, R., Garea, A., Fernández, I., Irabien, A., 2008. Resources reduction in the fluorine industry: fluoride removal and recovery in a fluidized bed crystallizer. Clean Technol. Environ. Policy 10, 203–210. https://doi.org/10.1007/s10098-007-0140-5.

Arters, D.C., Fan, L.-S., 1986. Solid-liquid mass transfer in a gas-liquid-solid fluidized bed. Chem. Eng. Sci. 41 (1), 107–115. https://doi.org/10.1016/0009-2509(86)85203-4.

Ballesteros, R.L., Riba, J.P., Couderc, J.P., 1982. Dissolution of non spherical particles in solid-liquid fluidization. Chem. Eng. Sci. 37 (11), 1639–1644. https://doi.org/10.1016/0009-2509(82)80034-1.

Bandosz, T.J., 2006. Activated Carbon Surfaces in Environmental remediation, 1st ed. Academic Press, New York, NY.

Bastiaan, T., 2020. The Origin of Carryover During Softening and its Influence on the Softening Process at Waternet. University of Utrecht, Department of Earth Sciences. Graduation Report.

Bögels, T., 2019. Calcite Growth Kinetics and Mechanisms During Water Softening. University of Utrecht, Department of Earth Sciences. Graduation Report.

Bošković, N., Grbavčić, Ž.B., Vuković, D.V., Marković-Grbavčić, M., 1994. Mass transfer between fluid and immersed surfaces in liquid fluidized beds of coarse spherical inert particles. Powder Technol. 79 (3), 217–225. https://doi.org/10.1016/0032-5910(94)02826-5.

Bošković-Vragolović, N., Garić Grulović, R., Grbavčić, Ž., 2007. Wall-to-liquid mass transfer in fluidized beds and vertical transport of inert particles. Journal of the Serbian Chemical Society 72 (11), 1103–1113. https://doi.org/10.2298/JSC0711103B.

Carman, P.C., 1937. Fluid flow through granular beds. Trans. Inst. Chem. Eng. 15, 32–48. https://doi.org/10.1016/S0263-8762(97)80003-2.

Chiou, E., 2018. An Improved Model of Calcium Carbonate Crystallization: An improved Kinetics-Model for the Calcium Carbonate Crystallization in the Fluidized Bed Softening Reactors at the Weesperkarspel Drinking Water Treatment plant. Delft University of Technology, Department of Civil Engineering and Geosciences. Master Thesis.

Crittenden, J.C., Trussell, R.R., Hand, D.W., Howe, K.J., Tchobanoglous, G., 2012. MWH's Water Treatment: Principles and Design, 3rd ed. John Wiley & Sons, New York, NY.

De Yoreo, J.J., Vekilov, P.G., 2003. Principles of crystal nucleation and growth. Rev. Mineral. Geochem. 54 (1), 57–93. https://doi.org/10.2113/0540057.

Derksen, J.J., 2014. Simulations of solid-liquid mass transfer in fixed and fluidized beds. Chem. Eng. J. 255, 233–244. https://doi.org/10.1016/j.cej.2014.06.067.

Di Felice, R., 1995. Review article number 47: of hydrodynamics of liquid fluidisation. Chem. Eng. Sci. 50 (8), 1213–1245. https://doi.org/10.1016/0009-2509(95)98838-6.

Eke, J., Yusef, A., Giwa, A., Sodiq, A., 2020. The global status of desalinization: an assessment of current desalinization technologies, plants and capacity. Desalinization 495, 114633. https://doi.org/10.1016/j.desal.2020.114633.

Ergun, S., 1952. Fluid flow through packed columns. Chem. Eng. Prog. 48 (2), 89–94.

Foscolo, P.U., Gibilaro, L.G., Waldram, S.P., 1983. A unified model for particulate expansion of fluidised beds and flow in fixed porous media. Chem. Eng. Sci. 38 (8), 1251–1260. https://doi.org/10.1016/0009-2509(83)80045-1.

Graveland, A., Van Dijk, J.C., De Moel, P.J., Oomen, J.H.C.M., 1983. Developments in water softening by means of pellet reactors. J. Am. Water Works Assoc. 75 (12), 619–625. https://doi.org/10.1002/j.1551-8833.1983.tb05247.x.

Gunn, D.J., 1978. Transfer of heat or mass to particles in fixed and fluidized beds. Int. J. Heat Mass Transf. 21 (4), 467–476. https://doi.org/10.1016/0017-9310(78)90080-7.

H2O waternetwerk, 2021. Waternet moet drinkwaterproductie flink opvoeren om in groeiende Amsterdamse vraag te voorzien. (2021, October 25). Retrieved from https://www.h2owaternetwerk.nl/h2o-actueel/waternet-moet-drinkwaterproductie-fors-uitbreiden.

Hammes, F., Boon, N., Vital, M., Ross, P., Magic-Knezev, A., Dignum, M., 2011. Bacterial colonization of pellet softening reactors used during drinking water treatment. Appl. Environ. Microbiol. 77 (3), 1041–1048. https://doi.org/10.1128/AEM.02068-10.

Hofman, J.A.M.H., Kramer, O.J.I., Van der Hoek, J.P., Nederlof, M.M., Groenendijk, M., 2006. Twenty years of experience with central softening in the Netherlands, water quality, environmental benefits and costs. In: Presented at the International Symposium On Health Aspects of Calcium and Magnesium in Drinking Water, Washington, DC.

Hu, R.Z., Huang, T.L., Wen, G., Yang, S.Y., 2017. Modelling particle growth of calcium carbonate in a pilot-scale pellet fluidized bed reactor. Water Sci. Technol. Water Supply 17 (3), 643–651. https://doi.org/10.2166/ws.2016.158.

Kalaga, D.V., Dhar, A., Dalvi, S.V., Joshi, J.B., 2014. Particle-liquid mass transfer in solid-liquid fluidized beds. Chem. Eng. J. 245, 323–341. https://doi.org/10.1016/j.cej.2014.02.038.

Kramer, O.J.I., 2021. Hydraulic Modelling of Liquid-Solid Fluidisation in Drinking Water Treatment Processes. Delft University of Technology, Department of Civil Engineering and Geosciences. Doctoral Dissertation.

Kramer, O.J.I., De Moel, P.J., Padding, J.T., Baars, E.T., El Hasadi, Y.M., Boek, E.S., Van der Hoek, J.P., 2020. Accurate voidage prediction in fluidisation systems for full-scale drinking water pellet softening reactors using data driven models. J. Water Process Eng. 37, 101481. https://doi.org/10.1016/j.jwpe.2020.101481.

Kunii, D., Levenspiel, O., 1969. Fluidization Engineering, 1st ed. John Wiley & Sons, New York, NY, p. 197.

Mahasti, N.N.N., Shih, Y.-J., Vu, X.-T., Huang, Y.H., 2017. Removal of calcium hardness from solution by fluidized-bed homogeneous crystallization (FBHC) process. J. Taiwan Inst. Chem. Eng. 78, 378–385. https://doi.org/10.1016/j.jtice.2017.06.040.

Micari, M., Moser, M., Cipollina, A., Tamburini, A., Micale, G., Bertsch, V., 2020. Towards the implementation of circular economy in the water softening industry: a technical economic and environmental analysis. J. Clean. Prod. 255, 120291. https://doi.org/10.1016/j.jclepro.2020.120291.

Mitchell, P., 2008. Central Heating, Installation, Maintenance and Repair. Brailsford Press, Eachwick, UK.

Nehrke, G., 2007. Calcite Precipitation from Aqueous Solution Transformation from Vaterite and Role of Solution Stoichiometry. University of Utrecht, Department of Earth Sciences. Doctoral Dissertation.

Palmen, L.J., Schetters, M.J.A., Van der Hoek, J.P., Kramer, O.J.I., Kors, L.J., Hofs, B., Koppers, H., 2014. Circular economy in drinking water treatment: reuse of grinded pellets as seeding material in the pellet-softening process. In: Poster session Presented At the IWA World Water Congress and Exhibition, Lisbon, Portugal, 21-26 September.

Richardson, J.F., Zaki, W.N., 1954. The sedimentation of a suspension of uniform spheres under conditions of viscous flow. Chem. Eng. Sci. 3 (2), 65–73. https://doi.org/10.1016/S0263-8762(97)80006-8.

Rietveld, L.C., 2005. Improving Operation of Drinking Water Treatment Through Modelling. Delft University of Technology. Doctoral Dissertation.

RoyalHaskoningDHV, 2024. Proven Crystallisation Technology For Purifying Water and Harvesting Valuable Resources. Retrieved from: https://www.royalhaskoningdhv.com/en/services/crystalactor.

Sand, K.K., Tobler, D.J., Dobberschütz, S., Larsen, K.K., Makvicky, E., Andersson, M.P., Wolthers, M., Stipp, S.L.S., 2016. Calcite growth kinetics: dependence on saturation

index, Ca^{2+}:CO_3^{2-} activity ratio, and surface atomic structure. Cryst. Growth Des. 16 (7), 3602–3612. https://doi.org/10.1021/acs.cgd.5b01792.
Schetters, M.J.A., Van der Hoek, J.P., Kramer, O.J.I., Kors, L.J., Palmen, L.J., Hofs, B., Koppers, H., 2015. Circular economy in drinking water treatment: reuse of ground pellets as seeding material in the pellet softening process. Water Sci. Technol. 71 (4), 479–486. https://doi.org/10.2166/wst.2014.494.
Seepma, S.Y.M.H., 2018. Revision of $CaCO_3$ Crystallization Kinetics in Drinking Water Softening. University of Utrecht, Department of Earth Sciences. Graduation Report.
Seepma, S.Y.M.H., Ruiz-Hernandez, S.E., Nehrke, G., Soetaert, K., Philipse, A.P., Kuipers, B.W.M., Wolthers, M., 2021. Controlling $CaCO_3$ Particle Size with $\{Ca^{2+}\}$:$\{CO_3^{2-}\}$ ratios in aqueous environments. Cryst. Growth Des. 21 (3), 1576–1590. https://doi.org/10.1021/acs.cgd.0c01403.
Sioson, A.S., Choi, A.E.S., De Luna, M.D.G., Huang, Y.H., Lu, M.C., 2019. Calcium carbonate granulation in a fluidized-bed reactor: kinetic, parametric and granule characterization analyses. Chem. Eng. J. 382, 122879. https://doi.org/10.1016/j.cej.2019.122879.
Sobhan, R., 2019. An Improved Kinetic Model and Optimized Configurations For Pellet softening: Modeling and Optimization of Pellet Softening Process in Drinking Water treatment. Master Thesis. Delft University of Technology, Department of Civil Engineering and Geosciences.
Stack, A.G., Grantham, M.C., 2010. Growth rate of calcite steps as a function of aqueous calcium-to-carbonate ratio: independent attachment and detachment of calcium and carbonate ions. Cryst. Growth Des. 10 (3), 1409–1413. https://doi.org/10.1021/cg901395z.
Tai, C.Y., Chien, W.-C., Chen, C.-Y., 1999. Crystal growth kinetics of calcite in a dense fluidized-bed crystallizer. Am. Inst. Chem. Eng. 45 (8), 1605–1614. https://doi.org/10.1002/aic.690450802.
Tang, C., 2019. Optimizing the Implementation of Drinking Water Softening. Technical University of Denmark, Department of Environmental Engineering. Doctoral Dissertation.
Tang, C., Hedegaard, M.J., Lopato, L., Albrechtsen, H.J., 2019. Softening of drinking water by the pellet reactor – Effects of influent water composition on calcium carbonate pellet characteristics. Sci. Total Environ. 652, 538–548. https://doi.org/10.1016/j.scitotenv.2018.10.157.
Tiangco, K.A.A., De Luna, M.D.G., Vilando, A.C., Lu, M.-C., 2019. Removal and recovery of calcium from aqueous solutions by fluidized-bed homogeneous crystallization. Process Saf. Environ. Prot. 128, 307–315. https://doi.org/10.1016/j.psep.2019.06.007.
Tournie, P., Laguerie, C., Couderc, J.P., 1977. Mass transfer in a liquid fluidized bed at low Reynolds numbers. Chem. Eng. Sci. 32 (10), 1259–1261. https://doi.org/10.1016/0009-2509(77)80062-6.
Tournie, P., Laguerie, C., Couderc, J.P., 1979. Correlations for mass transfer between fluidized spheres and a liquid. Chem. Eng. Sci. 34 (10), 1247–1255. https://doi.org/10.1016/0009-2509(79)85156-8.
Twort, A.C., Ratnayaka, D.D., Brandt, M.J., 2000. Water Supply, 5th ed. Butterworth-Heinemann, Oxford, UK.
Upadhyay, S.N., Tripathi, G., 1975. Liquid-phase mass transfer in fixed and fluidized beds of large particles. J. Chem. Eng. Data 20 (1), 20–26. https://doi.org/10.1021/je60064a001.
Van Ammers, M., Van Dijk, J.C., Graveland, A.J., Nuhn, P.A.N.M., 1986. State of the art of pellet softening in the Netherlands. Water Supply 4, 223–235.
Van Dijk, J.C., Wilms, D.A., 1991. Water treatment without waste material. Fundamentals and state of the art of pellet softening. J. Water Supply Res. Technol. AQUA 40 (5), 263–280.
Van Houwelingen, G., Bond, R., Seacord, T., Fessler, E., 2010. Experiences with pellet reactor softening as pretreatment for inland desalinization in the USA. Desalination Water Treat. 13 (1–3), 259–266. https://doi.org/10.5004/dwt.2010.1097.
Van Schagen, K.M., 2009. Model-Based Control of Drinking-Water Treatment Plants. Delft University of Technology. Doctoral Dissertation.
Van Schagen, K.M., Rietveld, L.C., Babuška, R., 2008a. Dynamic modelling for optimisation of pellet softening. J. Water Supply Res. Technol. AQUA, 57 (1), 45–56. https://doi.org/10.2166/aqua.2008.097.
Van Schagen, K.M., Rietveld, L.C., Babuška, R., Kramer, O.J.I., 2008b. Model-based operational constrains for fluidised bed crystallization. Water Res. 42 (1–2), 327–337. https://doi.org/10.1016//j.watres.2007.07.027.
Van den Hout, L., 2016. Modellering Van De hardheidsreductie: Optimalisatie van Het Hardheidsreductieproces Door Het Ontwikkelen Van Een Laagjesmodel Waarbij De Koppeling is Gemaakt Tussen Waterchemie En hydraulica. Graduation Thesis. Hogeschool Utrecht, Institute for Life Sciences and Chemistry.
Van der Bruggen, B., Goossens, H., Everard, P.A., Stemgée, K., Rogge, W., 2009. Cost-benefit analysis of central softening for production of drinking water. J. Environ. Manage. 91 (2), 541–549. https://doi.org/10.1016/j.jenvman.2009.09.024.
Van der Hoek, J.P., Hofman, J.A.M.H., Graveland, A.J., 1999. The use of biological activated carbon filtration for the removal of natural organic matter and organic micropollutants from water. Water Sci. Technol. 40 (9), 257–264. https://doi.org/10.1016/S0273-1223(99)00664-2.
Verdoes, D., Kashchiev, D., Van Rosmalen, G.M., 1992. Determination of nucleation and growth rates from induction times in seeded and unseeded precipitation of calcium carbonate. J. Cryst. Growth 118 (3–4), 401–413. https://doi.org/10.1016/0022-0248(92)90089-2.
Wen, C.Y., Yu, Y.H., 1966. A generalized method for predicting the minimum fluidization velocity. Am. Inst. Chem. Eng. 12 (3), 610–612. https://doi.org/10.1002/aic.690120343.
Wiechers, H.N.S., Sturrock, P., Marais, G.V.R., 1975. Calcium carbonate crystallization kinetics. Water Res. 9 (9), 835–845. https://doi.org/10.1016/0043-1354(75)90143-8.
Whitaker, S., 1972. Forced convection heat transfer correlations for flow in pipes, past flat plates, single cylinders, single spheres, and for flow in packed beds and tube bundles. Am. Inst. Chem. Eng. 18 (2), 361–371. https://doi.org/10.1002/aic.690180219.